JOURNAL OF PROPULSION AND POWER
Vol. 11, No. 3, May–June 1995

Solar Radiation on Mars: Stationary Photovoltaic Array

J. Appelbaum*
NASA Lewis Research Center, Cleveland, Ohio 44135
I. Sherman†
Tel-Aviv University, Ramat Aviv 69978, Israel
and
G. A. Landis‡
W. J. Schaffer Associates, Brook Park, Ohio 44142

Solar energy is an important power source for surface-based operation on Mars. Photovoltaic cells offer many advantages. Detailed information on solar radiation characteristics on Mars are necessary for effective design of future planned photovoltaic systems. In this article we present analytical expressions for solar radiation calculation and solar radiation data for inclined stationary flat surfaces for Mars as functions of day, latitude, and atmospheric dust load (optical depth). The diffuse component of the solar radiation on Mars due to the atmospheric dust can be significant, thus greatly affecting the optimal inclination angle of the photovoltaic array. The yearly optimal inclination angle for atmospheric optical depths measured by the Viking landers resulted in much smaller angles than the local latitudes.

Nomenclature

al	=	Mars surface albedo
G	=	global irradiance
G_{al}	=	irradiance due to albedo
G_b	=	beam irradiance
G_h, G_{bh}, G_{dh}	=	global, beam, and diffuse irradiance on a horizontal surface, respectively
G_β	=	global irradiance on an inclined surface
H, H_b, H_d, H_{al}	=	global, beam, diffuse, and albedo daily insolation
L_s	=	areocentric longitude, position of Mars in orbit around the sun
T	=	solar time, in hours, measured from midnight
T_d	=	number of daylight hours
z	=	zenith angle
α	=	solar altitude (or solar elevation), $\alpha = 90 - z$
β	=	inclination, the angle between the surface and the horizontal
β_p	=	optimal inclination angle of a surface for a given period
β_y	=	yearly optimal inclination angle of a surface
γ_c	=	surface azimuth angle
γ_s	=	solar azimuth, S zero, E negative, W positive
γ_{sr}, γ_{ss}	=	sunrise and sunset azimuth angles, respectively
δ	=	declination angle, the angular position of the sun at solar noon with respect to the plane of the equator
δ_p	=	average declination angle for a given period
θ	=	sun angle of incidence
τ	=	Mars optical depth
ϕ	=	geographic latitude, N positive, S negative
ω	=	hour angle, noon zero, morning negative, afternoon positive
ω_{cr}, ω_{cs}	=	sunrise and sunset hour angles on an inclined surface
ω_{sr}, ω_{ss}	=	sunrise and sunset hour angles, respectively

Received Sept. 30, 1993; revision received Feb. 3, 1994; accepted for publication Aug. 25, 1994.

*National Research Council–NASA Research Associate; currently Professor, Tel-Aviv University, Faculty of Engineering, Ramat Aviv 69978, Israel.

†Research Assistant, Faculty of Engineering.

‡Orbital Mechanics Engineer, NASA Lewis Research Center Group. Member AIAA.

Introduction

MISSIONS to the Mars surface will require electric power. Of the several possibilities, photovoltaic (PV) power systems can offer many advantages, including high power-to-weight ratio, modularity, and scalability. To design a photovoltaic system, detailed information on solar radiation data on the Martian surface is necessary.

The variation of the solar radiation on the Martian surface is governed by three factors: 1) the variation in Mars-sun distance, 2) variation in solar zenith angle due to Martian season and time of day, and 3) opacity of the Martian atmosphere.

A solar cell array mechanism may either be stationary or tracking. There are various configurations a stationary array (surface) may have. It may be horizontal, inclined with respect to ground, vertical, flat or curved; oriented toward the equator, toward E or any azimuth. A tracking array may track in two axes or in single axis of different kinds.

The solar radiation model for Mars and the solar radiation calculation procedure for horizontal surfaces have been published in Ref. 1. The present article is a continuation of Ref. 1 and deals with the solar radiation calculation on inclined, stationary-flat surfaces. Analytical expressions of solar angles and surface parameters are conveniently summarized. Some expressions may be found in the literature, some however, are new derivations. The solar expressions are in general forms and pertain to Mars as well as to the Earth. The solar radiation model, the procedure for solar radiation calculation, and the pertaining nomenclature for Mars will not be repeated in this article. The model assumes isotropic skies, therefore, the insolation on an inclined surface takes into account this type of distribution for the diffuse light.

The calculation of solar radiation reaching a surface involves trigonometric relationships between the position of the sun in the sky and the surface parameters. The global irradiance G, in W/m^2, on a surface is the sum of the direct beam irradiance G_b, the diffuse irradiance G_d, and the irradiance due to albedo G_{al}:

$$G = G_b + G_d + G_{al} \tag{1}$$

For a horizontal surface $G_{al} = 0$, and the irradiance is

$$G_h = G_{bh} + G_{dh} \tag{2}$$

For isotropic skies, the global irradiance G_β on an inclined surface with an angle β, is

$$G_\beta = G_b \cos\theta + G_{dh} \cos^2(\beta/2) + alG_h \sin^2(\beta/2) \tag{3}$$

where θ is the angle between the solar ray and the normal to the surface, al is the albedo.

As shown by Eq. (3), the irradiance on a surface is a function of θ and β. These two angles will be determined for all types of stationary surfaces.

Optimal inclination angle of a surface for clear skies may be determined based on the maximum beam irradiance or maximum daily beam insolation. The surface optimal inclination angle for days with appreciable diffuse irradiance ("cloudy" skies) may be determined based on the maximum daily global insolation.

Angles Involved in Solar Calculation

Position of the Sun on a Horizontal Surface

The angles involved in the position of the sun in the sky are shown in Fig. 1[2] and are defined in the Nomenclature.

The Mars day is 40 min, or about 2.75% longer than a terrestrial day. Hence, when expressed in terms of standard (terrestrial) hours, the relation between actual time T and hour angle ω is slightly different for Mars than for Earth. [In some earlier papers,[1] we have, for simplicity, expressed these equations in terms of "Mars hours" (H), defined by analogy to terrestrial hours (h) as 24 H = 1 sol. Thus, one Mars hour = 1.0275 h. In order that insolation values in kilowatt-hours to be expressed directly in terms of terrestrial hours, we have chosen here to use terrestrial hours rather than Mars hours. If the reader prefers to calculate in terms of Mars hours (i.e., Mars mean solar time), the relationship between hour angle and solar time is identical to that for Earth.] As shown in Fig. 2, the time (in terrestrial hours) and the hour angle ω are related by

$$\begin{aligned} &\text{Earth:} \quad \omega = 15T - 180 \\ &\text{Mars:} \quad \omega = 14.6T - 180 \end{aligned} \tag{4}$$

The solar zenith angle z is given by

$$\sin\alpha = \cos z = \sin\phi \sin\delta + \cos\phi \cos\delta \cos\omega \tag{5}$$

where δ is the declination, the angular position of the sun at solar noon with respect to the plane of the equator; for Earth -23.45 deg $\leq \delta \leq 23.45$ deg, $\delta = 0$ deg at vernal and autumnal equinoxes, $\delta = +23.45$ deg at summer solstice and -23.45 deg at winter solstice. For Mars: -24.936 deg $\leq \delta \leq 24.936$ deg.

The solar azimuth angle is related by[3]

$$\cot\gamma_s = (\sin\phi \cos\omega - \cos\phi \tan\delta)/\sin\omega \tag{6}$$

The sunrise and sunset hour angles are, respectively,

$$\omega_{sr} = -\cos^{-1}(-\tan\delta \tan\phi) \tag{7}$$

$$\omega_{ss} = \cos^{-1}(-\tan\delta \tan\phi) \tag{8}$$

for $|\phi| < \pi/2 - |\delta|$.

If $-\tan\delta \tan\phi > +1$, where $\phi < -\pi/2 + \delta$ or $\phi > \pi/2 + \delta$, the sun will neither rise nor set for the day: polar night.

If $-\tan\delta \tan\phi = \pm 1$, the sun will be on the horizon for an instant only.

If $-\tan\delta \tan\phi < -1$, where $\phi > \pi/2 - \delta$ or $\phi < -\pi/2 - \delta$, the sun will neither rise nor set for the day: polar day.

At the equator, $\phi = 0$; therefore $\omega_{sr} = \pi/2$, and the day length is independent of the solar declination (or season) and is always equal to 12 h (on Earth), or 12.33 h (on Mars).

At the equinoxes, $\delta = 0$; therefore $\omega_{sr} = \pi/2$, and the day length is independent of latitude and is equal to 12 h (Earth), or 12.33 h (Mars).

The sunrise and sunset azimuth angles are, respectively,

$$\sin\gamma_{sr} = \cos\delta \cos\omega_{sr} \tag{9}$$

$$\sin\gamma_{ss} = \cos\delta \cos\omega_{ss} \tag{10}$$

and the number of daylight hours is

$$\text{Earth:} \quad T_d = 2/15 \cos^{-1}(-\tan\delta \tan\phi) \tag{11}$$

$$\text{Mars:} \quad T_d = 0.137 \cos^{-1}(-\tan\delta \tan\phi) \tag{12}$$

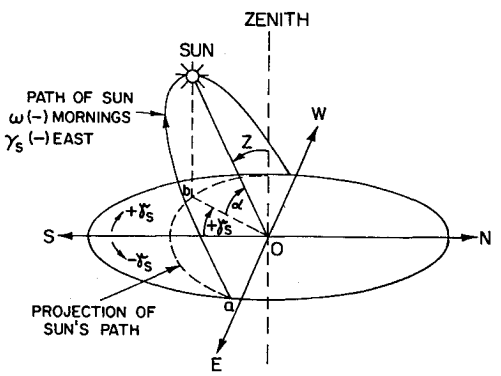

Fig. 1 Definition of angles for solar calculation.

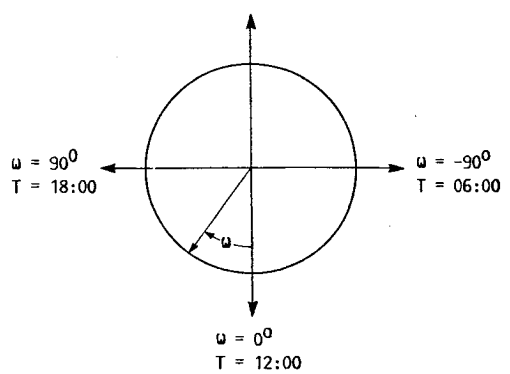

Fig. 2 Solar time and hour angle relation.

Solar Angles of an Inclined Surface

The solar angles involved on an inclined surface are shown in Fig. 3, where γ_c is the surface azimuth angle, the angle of the projection on a horizontal plane of the normal to the surface from the local meridian; zero S, E negative, W positive, -180 deg $\leq \gamma_c \leq 180$ deg, Fig. 4.

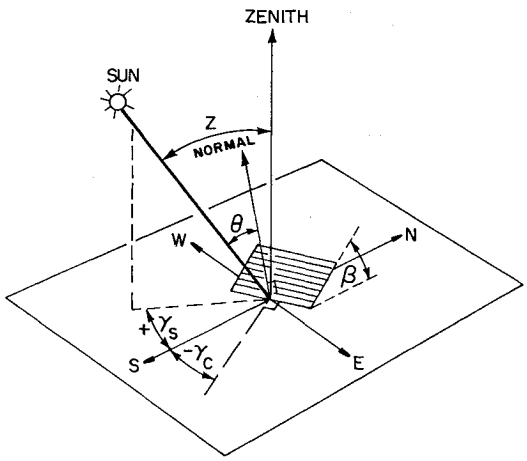

Fig. 3 Solar angles on an inclined surface.

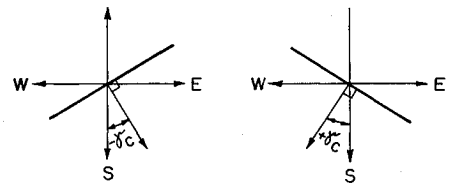

Fig. 4 Surface azimuth angle.

The sun angle of incidence on a surface in terms of the sun and surface angles can be written in the following two forms[2]:

$$\cos\theta = \cos\beta\cos z + \sin\beta\sin z\cos(\gamma_s - \gamma_c) \quad (13)$$

or

$$\cos\theta = \sin\delta\sin\phi\cos\beta - \sin\delta\cos\phi\sin\beta\cos\gamma_c + \cos\delta\cos\phi\cos\beta\cos\omega + \cos\delta\sin\phi\sin\beta \times \cos\gamma_c\cos\omega + \cos\delta\sin\beta\sin\gamma_c\sin\omega \quad (14)$$

The sunrise ω_{cr} and sunset ω_{cs} hour angles on an inclined surface that is oriented toward the E, $\gamma_c < 0$, Fig. 4, is given by

$$\omega_{cr} = -\min\{|\omega_{sr}|, \cos^{-1}[(-xy - \sqrt{x^2 - y^2 + 1})/(x^2 + 1)]\} \quad (15)$$

$$\omega_{cs} = \min\{\omega_{ss}, \cos^{-1}[(-xy + \sqrt{x^2 - y^2 + 1})/(x^2 + 1)]\} \quad (16)$$

and for a surface that is oriented toward the W, $\gamma_c > 0$, Fig. 4, the angles are

$$\omega_{cr} = -\min\{|\omega_{sr}|, \cos^{-1}[(-xy + \sqrt{x^2 - y^2 + 1})/(x^2 + 1)]\} \quad (17)$$

$$\omega_{cs} = \min\{\omega_{ss}, \cos^{-1}[(-xy - \sqrt{x^2 - y^2 + 1})/(x^2 + 1)]\} \quad (18)$$

where

$$x = (\cos\phi/\sin\gamma_c\tan\beta) + (\sin\phi/\tan\gamma_c) \quad (19)$$

$$y = \tan\delta[(\sin\phi/\sin\gamma_c\tan\beta) - (\cos\phi/\tan\gamma_c)] \quad (20)$$

The zenith angles at sunrise and sunset z_{cr}, z_{cs} on the surface are given by Eqs. (5) and (15–20).

For summer $|\omega_{sr}| \geq |\omega_{cr}|$, and $\omega_{ss} \geq \omega_{cs}$; and for winter $|\omega_{sr}| \leq |\omega_{cr}|$, and $\omega_{ss} \leq \omega_{cs}$ for a surface oriented toward the equator. Therefore, the actual sunrise or sunset hour angles on an inclined surface are determined by finding the minima

$$\omega_{cr} = \min(|\omega_{sr}|, |\omega_{cr}|) \quad (21)$$

$$\omega_{cs} = \min(\omega_{ss}, \omega_{cs}) \quad (22)$$

respectively.

Solar Angles of a Vertical Surface

θ on a vertical surface, is given by Eq. (13) or (14) for $\beta = 90$ deg, i.e.,

$$\cos\theta = \sin z(\cos\gamma_s\cos\gamma_c + \sin\gamma_s\sin\gamma_c) \quad (23)$$

or

$$\cos\theta = (\sin\phi\cos\delta\cos\omega - \cos\phi\sin\delta)\cos\gamma_c + \cos\delta\sin\omega\sin\gamma_c \quad (24)$$

The sunrise and sunset hour angles on the surface are given by Eqs. (15–20), where now

$$x = \sin\phi/\tan\gamma_c \quad (25)$$

$$y = -\tan\delta(\cos\phi/\tan\gamma_c) \quad (26)$$

Surface Facing the Equator

θ on an inclined surface β, facing the equator ($\gamma_c = 0$), is given by

$$\cos\theta = \cos\beta\cos z + \sin\beta\sin z\cos\gamma_s \quad (27)$$

or

$$\cos\theta = \sin\delta\sin(\phi - \beta) + \cos\delta\cos(\phi - \beta)\cos\omega \quad (28)$$

For the particular case of $\beta = \phi$, we have

$$\cos\theta = \cos\delta\cos\omega \quad (29)$$

The sunrise ω_{cr} and sunset ω_{cs} hour angles on the inclined surface facing the equator are

$$\omega_{cr} = -\cos^{-1}[-\tan\delta\tan(\phi - \beta)] \quad (30)$$

$$\omega_{cs} = \cos^{-1}[-\tan\delta\tan(\phi - \beta)] \quad (31)$$

Optimal Angles

Clear Skies

For clear days, the solar irradiance is symmetrical around noon and is maximum at true solar noon, $\omega = 0$. The optimal angles γ_c and β of the surface are usually determined based on the direct beam irradiance at noon for a clear day, i.e., results that are obtained from the differentiation of Eq. (14) with respect to γ_c and β at $\omega = 0$. The optimal azimuth of the surface is therefore

$$\gamma_c = 0 \quad (32)$$

i.e., the surface is facing S in the northern hemisphere, or facing N in the southern hemisphere. The optimal inclination angle is

$$\beta = \phi - \delta \quad (33)$$

i.e., the surface is normal to the sun rays at solar noon.

The solar incidence angle becomes [Eq. (28)]

$$\cos\theta = \sin^2\delta + \cos^2\delta\cos\omega \quad (34)$$

The solar declination angle varies daily, and for a stationary surface an average declination angle δ is used. Equation (33) thus becomes

$$\beta_p = \phi - \delta_p \tag{35}$$

where δ_p is the average declination angle for a given period p, and β_p is the optimal inclination angle for that period. The yearly average declination angle is $\delta_p = 0$, and Eq. (35) becomes

$$\beta_y = \phi \tag{36}$$

Substituting $\beta = \phi$ in Eq. (28), the angle of incidence becomes

$$\cos\theta = \cos\delta\cos\omega \tag{37}$$

A better approximation for the optimal angles γ_c and β of the surface is obtained based on the daily beam insolation on the surface from sunrise to sunset, i.e., $(12.33/\pi)\int_{\omega_{cr}}^{\omega_{cs}} G_b \cos\theta\, d\omega$. (The factor 12.33 accounts for the 24.66 h Mars day; for Earth this factor is exactly 12.) A clear day is assumed for the calculation, symmetrical around noon, and with a sinusoidal variation of the beam irradiance. Differentiation of the daily beam insolation with respect to γ_c and β we obtain

$$\gamma_c = 0 \tag{38}$$

$$\tan\beta = \frac{\cos\omega_{cr}\sin\phi\cos\delta - [1 - (2\omega_{cr}/\pi)^2]\cos\phi\sin\delta}{\cos\omega_{cr}\cos\phi\cos\delta + [1 + (2\omega_{cr}/\pi)^2]\sin\phi\sin\delta} \tag{39}$$

where ω_{cr} is given by Eq. (30). For winter

$$\min(|\omega_{sr}|, |\omega_{cr}|) = \omega_{sr}$$

The sun hour angle ω_{cr} on the surface is by itself a function of β, and since the β for summer is small, we may, with a good approximation, replace ω_{cr} by ω_{sr} [Eqs. (8) and (30)]. Equation (39) may now be written as

$$\tan\beta = \frac{\cos\omega_{sr}\sin\phi\cos\delta - [1 - (2\omega_{sr}/\pi)^2]\cos\phi\sin\delta}{\cos\omega_{sr}\cos\phi\cos\delta + [1 + (2\omega_{sr}/\pi)^2]\sin\phi\sin\delta} \tag{40}$$

Cloudy Skies

For days with high optical depth ("cloudy" skies) or days with appreciable diffuse irradiance, the surface optimal inclination angle may be determined by all three components of the solar irradiance. The daily global insolation H_β in Wh/m^2-day is given [see Eq. (3)] by

$$H_\beta = \frac{12.33}{\pi}\int_{\omega_{cr}}^{\omega_{cs}} [G_b\cos\theta + G_{dh}\cos^2(\beta/2) + alG_h\sin^2(\beta/2)]\, d\omega \tag{41}$$

In this section we will determine the surface optimal inclination angle for stationary surfaces. For isotropic skies, the optimal azimuth angle is at $\gamma_c = 0$, and θ is given by Eq. (28). The optimal inclination angle is obtained from the differentiation of Eq. (41) with respect to β. ω_{cr} and ω_{cs} depend on β [see Eqs. (30) and (31)], therefore, the evaluation of the derivative becomes complicated. However, as a good approximation, ω_{cr} and ω_{cs} may be replaced by ω_{sr} and ω_{ss}, respectively. The optimal β is obtained from

$$\frac{\partial H_\beta}{\partial\beta} = \int_{\omega_{sr}}^{\omega_{ss}} G_b\frac{\partial(\cos\theta)}{\partial\beta}\, d\omega + \frac{1}{2}\sin\beta\int_{\omega_{sr}}^{\omega_{ss}} (alG_h - G_{dh})\, d\omega = 0 \tag{42}$$

and by using Eq. (28), the daily optimal inclination angle becomes

$$\tan\beta = \frac{\sin\phi\cos\delta\int_{\omega_{sr}}^{\omega_{ss}} G_b\cos\omega\, d\omega - \cos\phi\sin\delta\int_{\omega_{sr}}^{\omega_{ss}} G_b\, d\omega}{\frac{1}{2}\int_{\omega_{sr}}^{\omega_{ss}} (G_{dh} - alG_h)\, d\omega + \sin\phi\sin\delta\int_{\omega_{sr}}^{\omega_{ss}} G_b\, d\omega + \cos\phi\cos\delta\int_{\omega_{sr}}^{\omega_{ss}} G_b\cos\omega\, d\omega} \tag{43}$$

Solar Radiation on an Inclined Stationary Surface

The expressions for the solar angles given in the previous section and the solar radiation model, Ref. 1, will now be applied to several possible photovoltaic array installations on the Martian surface.

The calculation of the solar irradiance on an inclined surface is based on the beam irradiance G_b, and on the global and diffuse irradiances G_h and G_{dh} on a horizontal surface, respectively, as given by Eq. (3). The daily global insolation on an inclined surface with an angle β is given by Eq. (41).

ω_{cr} and ω_{cs} are given in Eqs. (15–22), respectively. θ is a function of the γ_c and β angles.

Surface Facing the Equator

The optimal surface inclination angle may be determined for clear skies based on the beam irradiance (or daily beam insolation), or based on the daily global insolation. The yearly optimal inclination angle of a surface is given by Eq. (36), i.e.,

$$\beta_y = \phi \tag{44}$$

and the sun incident angle is given by Eq. (37), i.e.,

$$\cos\theta = \cos\delta\cos\omega \tag{45}$$

Table 1 gives the daily global insolation H for a Martian year for $\beta = \phi$ in kWh/m^2-day at Viking landers locations VL1 (ϕ = 22.3°N) and VL2 (ϕ = 47.7°N) for the measured opacities by the Viking lander cameras.[1] The season is indicated by the value of L_s areocentric longitude of the sun, measured in the orbital plane of the planet from its vernal equinox, $L_s = 0$ deg. The insolation is broken down into the beam H_b, diffuse H_d, and albedo H_{al} components. The variation of the global insolation is also shown in Fig. 5. The difference in the daily insolation between a horizontal and an inclined surface for $\beta = \phi$ at VL1 and VL2 is shown in Fig. 6 as a percentage gain (or loss) compared to the horizontal surface.[1] Figure 7 shows the insolation at VL1 and VL2 on an inclined surface, $\beta = \phi$, for clear skies with atmospheric optical depth of τ = 0.5. The effect of the global storms (L_s = 180 deg ÷ 360 deg) can be noticed by comparing Figs. 5 and 7.

The variation of the global insolation for the entire planet for inclined surfaces $\beta = \phi$, at local latitudes, may be of interest. For this purpose we resort to the optical depth model $\tau(\phi, L_s)$.[1] The results are shown in Fig. 8. It is also interesting to know the insolation for the entire planet for clear skies throughout the year. Figure 9 shows the insolation on inclined surfaces $\beta = \phi$, at local latitudes for τ = 0.5.

The optimal inclination angle of a surface will now be determined based on the insolation rather than on the irradiance using Eq. (43). The yearly optimal inclination angle resulted

Table 1 Daily insolation (H, H_b, H_d, and H_{al}) on an inclined surface for $\beta = \phi$ at VL1 and VL2

	VL1				VL2			
L_s	H	H_b	H_d	H_{al}	H	H_b	H_d	H_{al}
0	3355.0	1723.6	1604.5	26.9	2198.5	958.6	1160.1	79.8
5	3084.0	1247.0	1811.8	25.2	2628.9	1420.8	1116.3	91.8
10	3251.4	1513.4	1711.4	26.6	2909.2	1734.4	1073.9	100.9
15	3413.9	1829.2	1556.6	28.1	2565.5	1183.7	1285.5	96.3
20	3350.4	1705.0	1617.6	27.8	2872.2	1535.6	1230.0	106.6
25	3339.6	1692.1	1619.5	28.0	2787.6	1341.8	1338.5	107.3
30	3424.9	1901.7	1494.2	29.0	2918.2	1467.1	1337.6	113.5
35	3357.1	1767.1	1561.4	28.6	3260.4	1978.6	1155.6	126.2
40	3430.7	1980.6	1420.5	29.6	3361.8	2127.0	1102.4	132.4
45	3278.3	1625.4	1624.6	28.3	3312.9	1979.0	1200.1	133.8
50	3221.9	1513.2	1680.7	28.0	2919.9	1231.5	1566.2	122.2
55	3052.8	1177.2	1849.1	26.5	3353.0	1971.8	1240.6	140.6
60	3200.3	1485.0	1687.2	28.1	3370.6	1968.1	1259.0	143.5
65	3231.7	1565.4	1637.7	28.6	3387.8	1965.2	1276.4	146.2
70	3267.6	1656.9	1581.6	29.1	3455.0	2096.3	1207.5	151.2
75	3307.8	1757.3	1520.8	29.7	3471.3	2096.8	1221.1	153.4
80	3313.8	1755.8	1528.2	29.8	3395.8	1847.6	1398.0	150.2
85	3327.1	1760.2	1536.9	30.0	3509.8	2108.7	1244.3	156.8
90	3273.9	1566.0	1678.6	29.3	3532.3	2120.7	1253.6	158.0
95	3261.3	1485.7	1746.5	29.1	3557.0	2137.1	1261.0	158.9
100	3290.7	1501.7	1759.7	29.3	3487.2	1897.3	1435.6	154.3
105	3478.2	1944.3	1502.6	31.3	3511.2	1917.2	1439.6	154.4
110	3520.6	1973.9	1515.1	31.6	3534.5	1939.2	1441.2	154.1
115	3643.8	2273.0	1338.0	32.8	3723.5	2390.1	1172.1	161.3
120	3701.4	2318.9	1349.4	33.1	3872.3	2773.3	933.1	165.9
125	3761.4	2366.6	1361.4	33.4	3849.3	2633.6	1054.5	161.4
130	3822.7	2416.5	1372.5	33.7	3883.0	2674.7	1049.0	159.3
135	3884.5	2467.1	1383.5	33.9	3993.7	2913.3	920.6	159.8
140	3998.8	2684.4	1279.8	34.6	3852.2	2559.9	1141.2	151.1
145	3896.3	2260.5	1602.5	33.3	3955.8	2782.9	1022.5	150.4
150	3775.3	1903.6	1839.8	31.9	3861.6	2603.5	1114.3	143.8
155	3809.6	1930.3	1847.4	31.9	3850.2	2613.5	1097.3	139.4
160	3776.8	1832.7	1912.7	31.4	3950.3	2834.4	978.6	137.3
165	3794.3	1847.4	1915.6	31.3	3657.3	2395.0	1135.7	126.6
170	3739.3	1740.7	1968.5	30.6	3593.8	2365.8	1107.0	121.0
175	3735.8	1741.7	1963.8	30.3	2829.0	1376.8	1350.6	101.6
180	3721.1	1736.1	1955.0	30.0	2231.3	778.4	1368.1	84.8
185	3317.1	1159.8	2130.4	26.9	1868.8	505.0	1290.5	73.3
190	3104.8	934.7	2144.9	25.2	2094.9	798.2	1220.3	76.4
195	3161.0	1041.2	2094.3	25.5	2099.5	889.3	1136.6	73.6
200	3217.1	1161.3	2030.2	25.6	1797.1	657.4	1075.0	64.7
205	2372.6	328.6	2013.7	30.3	1130.4	162.6	915.7	52.1
210	1956.4	137.4	1789.5	29.5	855.4	49.9	752.4	53.1
215	2052.8	191.4	1830.9	30.5	816.2	60.4	710.6	45.2
220	2030.8	204.1	1798.0	28.7	739.4	52.3	647.2	39.9
225	2007.7	218.6	1762.1	27.0	685.5	51.5	599.2	34.8
230	2043.8	273.3	1745.9	24.6	877.5	207.3	637.0	33.2
235	2027.8	297.5	1707.4	22.9	625.5	70.7	528.9	25.9
240	2025.7	326.9	1677.3	21.5	520.5	35.2	461.2	24.1
245	2068.8	393.1	1656.0	19.7	629.0	117.9	486.6	24.5
250	2125.1	479.8	1627.4	17.9	529.1	70.8	436.8	21.5
255	2221.1	594.5	1609.2	17.4	406.4	21.3	366.7	18.4
260	2180.2	578.9	1584.2	17.1	401.6	26.2	358.2	17.2
265	1899.1	342.7	1538.3	18.1	442.4	49.5	374.7	18.2
270	1670.1	189.6	1460.4	20.1	335.7	7.8	310.3	17.6
275	1354.1	60.9	1272.7	20.5	307.6	2.8	285.7	19.1
280	1206.9	32.8	1155.8	18.3	300.1	1.5	278.0	20.6
285	1330.7	54.8	1255.8	20.1	321.1	2.6	297.5	21.0
290	1026.8	12.3	998.8	15.7	332.8	2.4	307.6	22.8
295	1167.7	24.5	1125.4	17.8	339.2	1.8	312.9	24.5
300	1260.6	36.0	1205.4	19.2	380.7	3.4	350.1	27.2
305	1451.5	71.1	1358.5	21.9	441.8	8.7	404.4	28.7
310	1728.7	160.8	1543.4	24.5	519.9	20.9	468.9	30.1
315	2052.7	357.6	1673.3	21.8	831.5	174.1	625.1	32.3
320	2250.1	504.1	1725.3	20.7	1201.4	449.2	711.0	41.2
325	2343.4	566.4	1756.2	20.8	1208.9	401.4	764.2	43.3
330	2479.9	679.3	1780.3	20.3	1331.7	458.7	825.3	47.7
335	2628.3	808.2	1799.1	21.0	1345.7	417.0	878.8	49.9
340	2581.6	726.0	1834.3	21.3	1076.1	154.7	870.0	51.4
345	3044.0	1281.2	1738.7	24.1	1645.4	578.4	1006.5	60.5
350	2908.0	1062.7	1821.9	23.4	1828.9	696.9	1065.3	66.7
355	3158.7	1403.9	1729.5	25.3	2243.0	1085.5	1079.5	78.0
360	3355.0	1723.6	1604.5	26.9	2198.5	958.6	1160.1	79.8
Average	2841.0	1171.4	1643.2	26.3	2179.4	1153.0	937.9	88.5

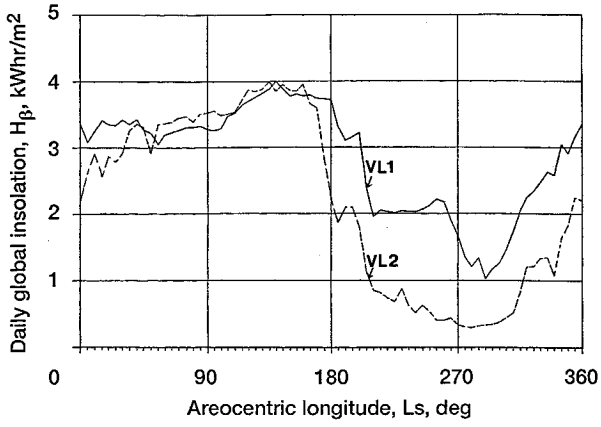

Fig. 5 Variation of daily global insolation on an inclined surface $\beta = \phi$, at VL1 and VL2.

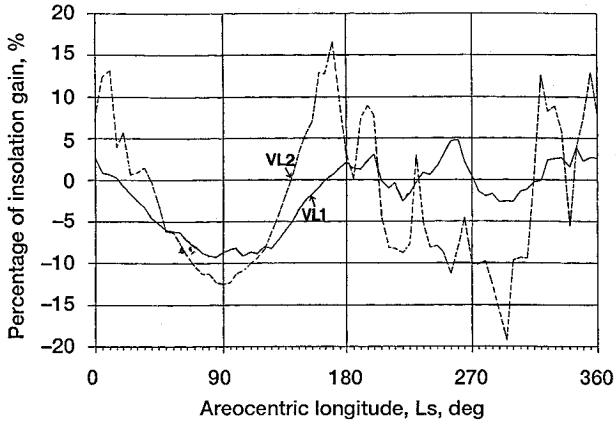

Fig. 6 Percentage of daily global insolation loss (gain) on an inclined surface $\beta = \phi$, as compared to a horizontal surface at VL1 and VL2.

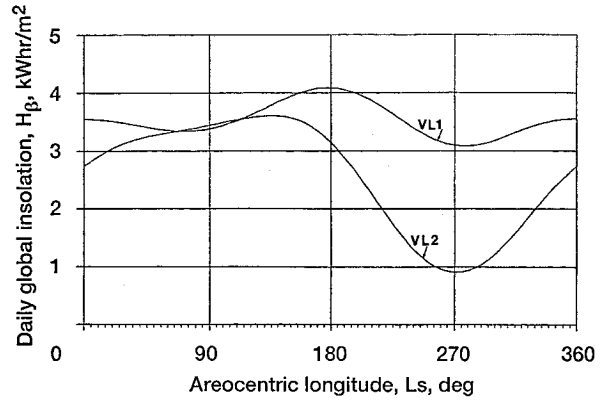

Fig. 7 Variation of daily global insolation on an inclined surface $\beta = \phi$, at VL1 and VL2 for optical depth of 0.5.

in 6.5 deg at VL1, and 22 deg at VL2 for the measured opacities. Table 2 gives the daily direct beam, diffuse and the albedo components, as well as the daily global insolation for the optimal inclination angles at VL1 and VL2. By comparing Tables 1 and 2 we obtain the percentage gain in the yearly insolation for the two installations: the approximate ($\beta = \phi$) and the exact optimal angles [Eq. (43)]. The gain in the yearly global insolation is 2.47% at VL1 and 6.46% at VL2 in favor of the exact inclination angle.

Vertical Surface

A special case is a vertical surface, i.e., $\beta = 90$ deg. A vertical bifacial surface (two-sided surface) acting as a PV

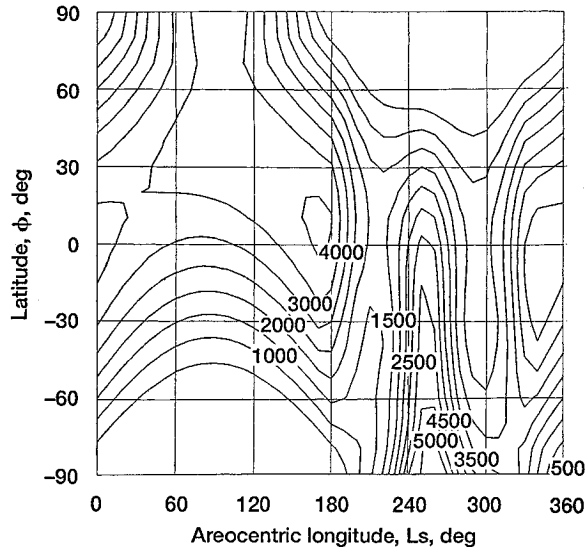

Fig. 8 Variation of daily global insolation H_β (Wh/m^2) with latitude and areocentric longitude on an inclined surface $\beta = \phi$, based on the optical depth function [1, Eq. (1)].

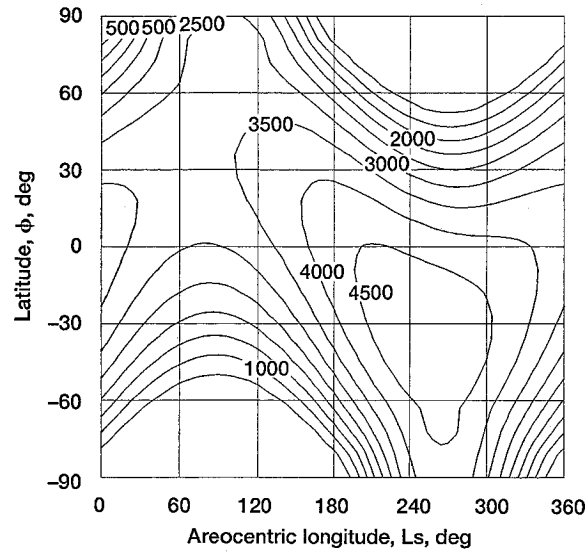

Fig. 9 Variation of daily global insolation H_β (Wh/m^2) with latitude and areocentric longitude on an inclined surface $\beta = \phi$, for optical depth of 0.5.

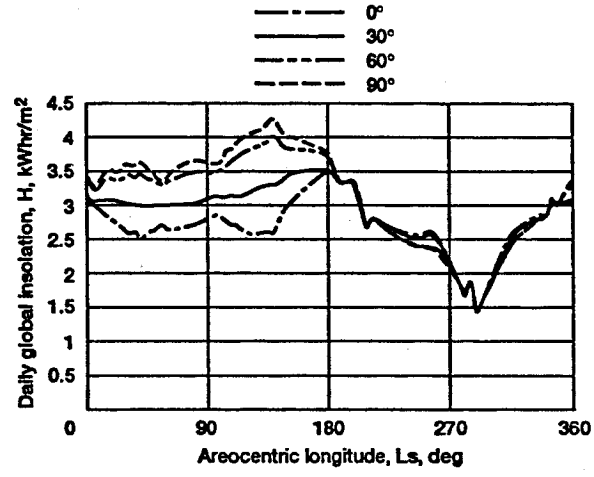

Fig. 10 Variation of daily global insolation on a bifacial vertical surface at different azimuth angles γ_c at VL1.

Table 2 Daily insolation (H, H_b, H_d, and H_{al}) on optimal inclined surfaces with angles β_{VL1} = 6.5 deg and β_{VL2} = 22 deg at VL1 and VL2, respectively

	VL1 beta optimal = 6.5 deg				VL2 beta optimal = 22.0 deg			
L_s	H	H_b	H_d	H_{al}	H	H_b	H_d	H_{al}
0	3322.7	1658.4	1662.0	2.3	2217.9	863.8	1336.3	17.8
5	3093.4	1214.9	1876.3	2.2	2614.6	1308.0	1286.2	20.4
10	3267.8	1493.4	1772.1	2.3	2891.9	1632.6	1236.8	22.5
15	3443.1	1829.1	1611.6	2.4	2638.6	1136.0	1481.2	21.4
20	3404.5	1725.7	1676.4	2.4	2948.4	1507.4	1417.3	23.7
25	3413.1	1733.6	1677.1	2.4	2908.4	1342.9	1541.6	23.9
30	3523.5	1973.7	1547.3	2.5	3066.1	1499.7	1541.1	25.3
35	3473.2	1854.4	1616.3	2.5	3434.3	2075.2	1331.0	28.1
40	3578.7	2104.8	1471.3	2.6	3580.1	2280.1	1270.5	29.5
45	3427.4	1741.6	1683.3	2.5	3570.0	2158.1	1382.2	28.8
50	3378.5	1635.7	1740.4	2.4	3182.0	1350.0	1804.8	27.2
55	3197.4	1280.4	1914.7	2.3	3684.7	2224.8	1428.6	31.3
60	3383.4	1633.5	1747.5	2.4	3735.8	2253.1	1450.7	32.0
65	3436.0	1737.2	1696.3	2.5	3782.2	2279.0	1470.6	32.6
70	3491.6	1850.8	1638.3	2.5	3889.1	2464.9	1390.5	33.7
75	3552.4	1974.5	1575.3	2.6	3927.9	2487.0	1406.8	34.1
80	3566.2	1980.4	1583.2	2.6	3836.9	2192.9	1610.5	33.5
85	3584.4	1989.5	1592.3	2.6	3995.1	2526.7	1433.5	34.9
90	3508.2	1766.6	1739.1	2.5	4023.9	2544.5	1444.2	35.2
95	3484.7	1672.9	1809.3	2.5	4048.9	2560.7	1452.8	35.4
100	3512.8	1687.4	1822.9	2.5	3940.2	2251.9	1653.9	34.4
105	3747.1	2187.8	1556.6	2.7	3954.3	2261.4	1658.5	34.4
110	3782.9	2210.7	1569.5	2.7	3961.8	2267.8	1659.7	34.3
115	3928.2	2539.3	1386.1	2.8	4174.1	2787.7	1350.5	35.9
120	3970.0	2569.4	1397.7	2.9	4325.5	3213.1	1075.5	36.9
125	4011.7	2599.4	1409.4	2.9	4345.9	2996.0	1214.0	35.9
130	4052.8	2628.8	1421.1	2.9	4236.1	2991.3	1209.3	35.5
135	4093.4	2656.5	1434.0	2.9	4305.0	3209.3	1060.1	35.6
140	4190.7	2862.0	1325.7	3.0	4099.2	2750.2	1315.3	33.7
145	4037.4	2375.6	1658.9	2.9	4147.5	2936.4	1177.6	33.5
150	3881.4	1973.5	1905.1	2.8	3999.3	2683.2	1284.1	32.0
155	3893.5	1977.6	1913.1	2.8	3930.0	2635.5	1263.5	31.0
160	3839.2	1854.4	1982.1	2.7	3957.7	2799.1	1128.0	30.6
165	3832.4	1846.4	1983.3	2.7	3644.3	2307.3	1308.8	28.2
170	3758.7	1717.8	2038.3	2.6	3530.8	2228.9	1275.0	26.9
175	3733.6	1697.2	2033.8	2.6	2845.8	1267.1	1556.1	22.6
180	3698.1	1670.4	2025.1	2.6	2296.1	701.4	1575.8	18.9
185	3310.8	1102.1	2206.4	2.3	1949.0	445.9	1486.8	16.3
190	3100.8	877.6	2221.0	2.2	2113.2	690.1	1406.1	17.0
195	3136.4	965.4	2168.1	2.2	2078.5	752.9	1309.2	16.4
200	3167.3	1063.4	2101.7	2.2	1798.5	545.6	1238.5	14.4
205	2386.8	298.1	2086.1	2.6	1199.5	132.7	1055.2	11.6
210	1979.2	123.4	1853.2	2.6	918.5	40.0	866.7	11.8
215	2068.6	169.9	1896.1	2.6	876.6	47.5	819.0	10.1
220	2043.5	179.2	1861.8	2.5	794.5	40.4	745.2	8.9
225	2017.0	189.9	1824.8	2.3	737.1	39.0	690.4	7.7
230	2045.6	235.0	1808.5	2.1	895.1	154.0	733.7	7.4
235	2023.7	253.4	1768.3	2.0	667.0	51.8	609.4	5.8
240	2014.5	276.0	1736.6	1.9	562.1	25.5	531.2	5.4
245	2045.4	329.2	1714.5	1.7	650.0	84.0	560.6	5.4
250	2085.6	398.9	1685.2	1.5	557.8	49.9	503.1	4.8
255	2159.3	491.2	1666.6	1.5	441.6	14.9	422.6	4.1
260	2118.9	476.6	1640.8	1.5	434.9	18.2	412.9	3.8
265	1876.8	282.1	1593.1	1.6	470.1	34.3	431.7	4.1
270	1670.4	156.3	1512.4	1.7	366.7	5.4	357.4	3.9
275	1370.3	50.4	1318.1	1.8	335.3	1.9	329.1	4.3
280	1225.8	27.2	1197.0	1.6	326.0	1.1	320.3	4.6
285	1347.7	45.6	1300.4	1.7	349.4	1.9	342.8	4.7
290	1046.0	10.3	1034.3	1.4	361.1	1.7	354.3	5.1
295	1187.4	20.6	1165.3	1.5	367.3	1.3	360.5	5.5
300	1280.3	30.5	1248.1	1.7	411.8	2.5	403.2	6.1
305	1469.7	60.8	1407.0	1.9	478.8	6.4	466.0	6.4
310	1739.2	138.4	1598.7	2.1	562.4	15.6	540.1	6.7
315	2044.9	310.2	1732.8	1.9	859.0	131.6	720.2	7.2
320	2229.9	441.5	1786.6	1.8	1172.7	344.8	818.7	9.2
325	2322.0	501.5	1818.7	1.8	1204.4	314.1	880.7	9.6
330	2453.5	608.0	1843.7	1.8	1327.1	365.9	950.6	10.6
335	2597.5	731.7	1864.0	1.8	1363.3	339.4	1012.8	11.1
340	2566.2	665.3	1899.1	1.8	1142.5	128.8	1002.3	11.4
345	2989.8	1187.1	1800.6	2.1	1663.0	490.1	1159.4	13.5
350	2885.9	997.4	1886.5	2.0	1844.9	602.5	1227.5	14.9
355	3127.3	1333.8	1791.3	2.2	2218.8	957.7	1243.7	17.4
Average	2911.5	1207.4	1701.8	2.3	2320.4	1220.2	1080.5	19.7

array or as a radiator may be of special interest. The variation of the daily global insolation on a bifacial vertical surface is therefore calculated at different azimuth angles γ_c at VL1 for the observed opacities, and is shown in Fig. 10. The azimuth $\gamma_c = 0$ indicates that side A is facing S and side B is toward N. The figure shows that there is a small difference in the insolation for different azimuth angles at times with dust storms (L_s = 180 deg ÷ 360 deg) since the insolation is dictated mainly by the diffuse light, however, for clear skies the azimuth effects the global insolation. The best orientation for a PV array to face would be the E-W direction, and for a radiator the N-S direction.

Photovoltaic Array Considerations

In addition to the sunlight availability, operational considerations for Mars photovoltaic power systems include the low operating temperature, wind, dust, and the chemical environment of Mars. These are considered in Ref. 4 along with a discussion of the merits of various types of solar cells that may be used for power systems on Mars.[5]

The low operating temperatures will increase the cell conversion efficiency by a greater amount for cells with a higher temperature coefficient, and thus reduce the advantage in efficiency of GaAs solar cells over silicon. For example, at an operating temperature of 200 K (the peak daytime temperature at the VL1 site during the 1977b dust storm[4]), the power output of a silicon cell will increase by nearly 45%; whereas a GaAs cell will only increase by 20%.

The temperature cycling of the arrays during the Mars day/night cycle is also a consideration for array lifetimes. The temperature encountered is similar to the temperature extremes encountered by a solar array in geosynchronous orbit (GEO) during eclipse, but the cycle time is considerably slower (e.g., cooling from peak temperature to minimum temperature in about 12 h on Mars, vs 1 h in GEO). It is thus expected that an array designed to survive the temperature cycling environment of GEO should also survive Mars conditions.

The sunlight is also spectrally shifted (reddened) due to dust. The peak of the atmospheric transmission is about 0.8 μm,[6] and the amount of variation between peak and average transmission increases with atmospheric opacity and with zenith angle. This peak transmission is close to the peak spectral response wavelength of both silicon and GaAs solar cells, resulting in a slight increase in conversion efficiency.[7]

Dust accumulation on the cells by settling from the atmosphere may be a significant problem for long duration missions without a mechanism for clearing dust from the arrays. The dust deposition rate is estimated to result in an average decrease of 20–80% from initial power levels over the course of one Mars year,[8] depending on the number of dust storms. Actual arrays at a given location may have higher or lower amounts of obscuration, however, since the dust settling rate is believed to be strongly dependent on location. There may be removal of dust by wind as well as deposition. Although the Viking lander did not measure winds high enough to remove deposited dust, views from the Viking cameras showed a gradual darkening of the bright dust layers deposited on the surface following global storms, indicative of dust removal.

Several dust removal mechanisms can be envisioned. It may be desirable to design arrays with surfaces that can be raised to "flap" in the wind to shake dust free, or else arrays with naturally flexible surfaces. Alternately, an array surface that can be charged alternately to a large positive and then negative potential to remove dust by electrostatic repulsion is a possibility.

Finally, this analysis has discussed the total insolation over the course of a Mars day. For many applications, it is also useful to make the power profile during the day as flat as possible, in order to minimize the requirements for storage. In particular, it is important to maximize the power production near sunrise and sunset. One method to accomplish this with a fixed array is with the use of a "tent" array, with surface elements inclined toward the E and to the W.[9] This reduces the total insolation produced over the day, but increases the direct beam component of the insolation in the early morning and late evening. Thus, this is most effective in flattening the power profile for low optical depths.

Conclusions

Effective design and utilization of solar energy depend to a large extent on adequate knowledge of solar radiation characteristics in the region of solar energy system operation. This article deals with solar radiation calculation on inclined-stationary-flat-surfaces and is based on the solar radiation model developed in Ref. 1. The analytical expressions of the solar angles and surface parameters may be used for the calculation of the solar radiation on any desired inclined stationary surface planned for Mars missions. Insolation data for Mars are given at the Viking landers locations (Fig. 5) and for the entire planet (Fig. 9) at commonly used latitude-inclination angles, $\beta = \phi$. These data are compared to years without global dust storms assuming atmospheric optical depth of $\tau = 0.5$.

The commonly used latitude-inclination angle $\beta = \phi$ is derived based on the direct beam irradiance that dominates clear skies. For skies with appreciable diffuse insolation, the optimal inclination (Eq. 43) is smaller than $\beta = \phi$. The insolation for the yearly optimal inclination angle is shown in Table 2.

The solar radiation model for Mars [the normalized net flux function $f(z, \tau, al)$ and, consequently, the solar radiation expressions] assumes isotropic skies, i.e., the intensity of the sky diffuse radiation is assumed uniform over the sky dome. Isotropic skies may be a good approximation since the Martian atmosphere consists mainly of suspended dust particles. The dependence of the global, beam, and diffuse irradiances on τ and z are given by Eqs. (14–16) and are shown in Figs. 5–7 in Ref. 1.

The substitution of the sunrise ω_{sr} and sunset ω_{ss} hour angles for ω_{cr} and ω_{cs} in Eqs. (40) and (43) may be taken as a good approximation for not too high latitudes, since the insolation in the vicinity of the optimal inclination angles varies very moderately. One may, however, calculate the exact inclination angle β from Eq. (39), iteratively using Eq. (40) for the starting point. The insolation is calculated using ω_{cr} and ω_{cs} angles.

Acknowledgment

This work was funded under NASA Grant NAGW-2022.

References

[1]Appelbaum, J., Landis, G. A., and Sherman, I., "Solar Radiation on Mars Update 1991," *Solar Energy*, Vol. 50, No. 1, 1993, pp. 35–51.

[2]Iqbal, M., *An Introduction to Solar Radiation*, Academic Press, Toronto, 1983, Chap. 1.

[3]Sayigh, A. A., *Solar Energy Engineering*, Academic Press, New York, 1977, Chap. 2.

[4]Zurek, R. W., Barnes, J. R., Haberle, R. M., Pollack, J. B., Tillman, J. E., and Leovy, C. B., "Dynamics of the Atmosphere of Mars," *Mars*, Univ. of Arizona Press, Tucson, AZ, 1992, pp. 835–933.

[5]Landis, G. A., and Appelbaum, J., "Photovoltaic Power Options for Mars," *Space Power*, Vol. 10, No. 2, 1991, pp. 225–237.

[6]Haberle, R. M., et al., "Atmospheric Effects on the Utility of Solar Power on Mars," *Resources of Near Earth Space*, Univ. of Arizona Press, Tucson, AZ, 1993, pp. 845–885.

[7]Burger, D., "Solar Array Considerations for the Mars Surface," *Case for Mars V*, Boulder, CO, May 1993, pp. 26–29.

[8]Landis, G. A., "Instrumentation for Measurement of Dust Deposition on Solar Arrays on Mars," *Case for Mars V*, Univ. of Colorado, Boulder, CO, May 1993, pp. 27, 28.

[9]Landis, G. A., Bailey, S. G., Brinker, D. J., and Flood, D. J., "Photovoltaic Power for a Lunar Base," *Acta Astronautica*, Vol. 22, 1990, pp. 197–203.